Journal of the Korean Physical Society, Vol. 75, No. 12, December 2019, pp. 1033∼1037

Optimization of Hole Injection and Transport Layers for High-Performance Quantum-Dot Light-Emitting Diodes

Jae Seung Shin, Jong Hun Yu, Su Been Heo and Seong Jun Kang*
Department of Advanced Materials Engineering for Information and Electronics, Kyung Hee University, Yongin 17104, Korea

(Received 24 September 2019; accepted 7 October 2019)

High-luminance, efficient quantum-dot light-emitting diodes (QLEDs) have been achieved by optimizing the balance between the hole injection layer (HIL) and the hole transport layer (HTL). Different concentrations of vanadium oxide (V_2O_5) and poly[(9,9-dioctylfluorenyl-2,7-diyl)-co-(4,4'-(4-sec-butylphenyl)diphenylamine)] (TFB) solutions were used to form the efficient HIL and HTL, respectively, for the QLEDs. The hole injection and transport behavior was characterized by using hole-only devices (HODs). The QLEDs, which were prepared with 0.5 wt.% of V_2O_5 and 0.1 wt.% of TFB as HIL and HTL, respectively, showed a maximum current efficiency of 2.27 cd·A^{-1} and a maximum luminance of 71,260 cd·m^{-2}. Moreover, the turn-on voltage of the device was as low as 2.2 V due to the efficient carrier injection and transport. The results provide useful information for fabricating high-performance QLEDs.

PACS numbers: 81.07.Ta, 85.60.−q, 85.60.Bt, 85.60.Jb
Keywords: Quantum-dots, Light-emitting diodes, Hole injection layer, Hole transport layer, Optimization
DOI: 10.3938/jkps.75.1033

I. INTRODUCTION

Quantum dots (QDs) have been used in various optoelectronics, such as light-emitting diodes (LEDs), photodetectors, and solar cells, because of their superior electrical and optical characteristics [1–4]. Due to the quantum confinement effect, the optoelectrical properties of QDs can be controlled by varying their size, shape, and composition [5]. In particular, the emission wavelength of QD-based LEDs can be easily controlled with excellent color purity [6]. Generally, the full width at half maximum of the QDs is as narrow as <40 nm [7]. Therefore, QDs are widely used in displays, and quantum-dot light-emitting diodes (QLEDs) have been considered for next-generation displays [8,9].

Transition-metal oxides (TMOs) are inorganic materials that can be used in the hole injection layer (HIL) in QLEDs due to their high stability to oxygen, hydrogen, and heat [10, 11]. Among TMOs, vanadium oxide (V_2O_5) is a good candidate QLED HIL because it is processable in a low-temperature solution process [12]. Poly[(9,9-dioctylfluorenyl-2,7-diyl)-co-(4,4'-(4-sec-butylphenyl)diphenylamine)] (TFB) is widely used as a hole transport layer (HTL) in QLEDs [13]. It is known to have a higher hole mobility than other HTL materials, such as poly(9-vinylcarbazole) (PVK) and poly[bis(4-phenyl)(4-butylphenyl)amine] (poly-TPD) [14,15]. Meanwhile, the balance between hole and electron injection is a key factor affecting the device performance [16–18]. When the charge balance is inefficient, QDs are negatively charged, and a quenching effect of fluorescence occurs through a nonradiative Auger recombination process [19]. The key to improving the charge balance is inhibiting electron injection while enhancing hole injection into the device [20, 21]. One method is to insert an additional layer into the QLEDs to modify the balance of charge injection and transport [22]. Another way for improving the charge balance is composing a multilayer HIL to decrease the hole injection barrier [23]. Therefore, although V_2O_5 and TFB are a good combination when used as the HIL and HTL, respectively, a detailed study should be carried out to optimize the two layers such that efficient QLEDs based on a V_2O_5 HIL and a TFB HTL can be fabricated.

In this study, we changed the concentrations of the V_2O_5 and the TFB solutions to improve the hole injection and the transport behavior. Various mixtures of the vanadium precursor and isopropyl alcohol were prepared, and the TFB precursor was mixed into p-xylene at various concentrations. Hole-only devices (HODs) and electron-only devices (EODs) were fabricated to characterize the carrier injection and the transport behavior. The QLEDs, which were prepared with 0.5 wt.% of V_2O_5 and 0.1 wt.% of TFB as the HIL and the HTL, respectively, exhibited a maximum current efficiency of 2.27 cd·A^{-1} and a maximum luminance of 71,260 cd·m^{-2}.

*E-mail: junkang@khu.ac.kr

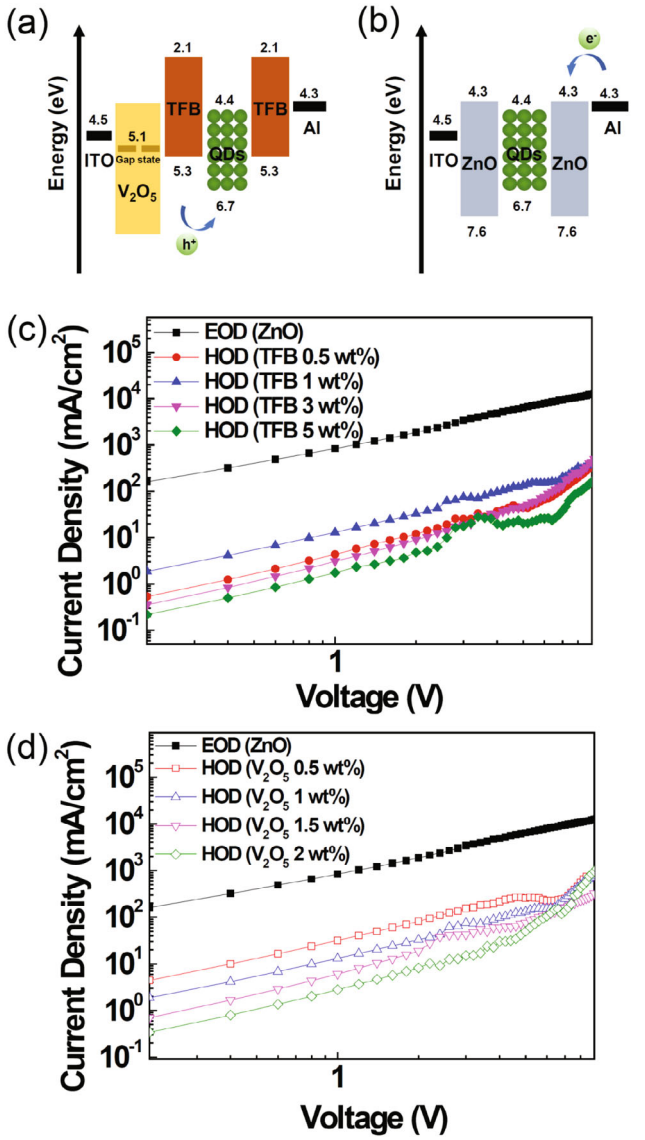

Fig. 1. (Color online) Energy level diagram for the (a) HODs and (b) EODs. J-V characteristics of the EODs (ITO/ZnO/QDs/ZnO/Al) and HODs (ITO/V_2O_5/TFB/QDs/TFB/Al) (c) with different TFB solutions and (d) with different V_2O_5 solutions.

Moreover, the turn-on voltage of the device was as low as 2.2 V due to the efficient carrier injection and transport. The reported results provide useful information for fabricating high-performance QLEDs.

II. EXPERIMENTS

Vanadium (V) triisopropoxide oxide (96%) liquid was purchased from Alfa Aesar (USA), and TFB was purchased from Lumtec (Taiwan). CdSe/ZnS QDs were obtained from UNIAM (Korea) while zinc oxide (ZnO) was purchased from Avantama (Switzerland). Isopropyl alcohol and p-xylene were purchased from Daejung (Korea) and Sigma-Aldrich (USA), respectively. The HTL solution was prepared by mixing the TFB precursor in a p-xylene (0.861g ml^{-1}) solution at different ratios, that is, 0.5:1, 1:1, 3:1, and 5:1, by weight. The HIL solution was prepared by mixing the vanadium precursor in an isopropyl alcohol solution in 0.5:1, 1:1, 1.5:1, and 2:1 ratios by weight. Both were stirred for 30 min under ambient conditions.

To fabricate the QLEDs, we cleaned a patterned indium-tin-oxide (ITO) glass substrate with acetone, isopropyl alcohol, and deionized water (DI water) in sequence in a sonicator. After sonication, the substrate was treated with ultraviolet ozone to increase its hydrophilicity and the work function of the ITO surface. The V_2O_5 solution was then spin-coated onto the ITO surface at 3,000 rpm for 30 s, followed by an annealing process at 25 °C for 15 min. The TFB solution was spin-coated onto the V_2O_5 layer at 3000 rpm for 30 s, followed by annealing at 180 °C for 30 min. The colloidal CdSe/ZnS QDs were spin-coated onto the surface of the TFB and annealed at 180 °C for 30 min. The entire procedure was carried out under ambient conditions. Finally, an aluminum cathode was deposited on the device by using a shadow mask and thermal evaporator. The current density - voltage (J-V) characteristics of the EODs and the HODs and the electroluminescence (EL) characteristics of the QLEDs were measured using a conventional current-voltage-luminance (I-V-L) measurement system (M6100, McScience, Korea) under ambient conditions.

III. RESULTS AND DISCUSSION

HODs were fabricated to characterize the hole transport behavior in the HIL and the HTL based on different concentrations of the V_2O_5 and the TFB solutions. EODs were also fabricated to compare the electron transport behaviors. The electronic structures of the HODs and the EODs were ITO/V_2O_5/TFB/QDs/TFB/Al and ITO/ZnO/QDs/ZnO/Al, as shown in Figs. 1(a) and 1(b), respectively. Values of the energy levels of ITO, V_2O_5, TFB, QDs, ZnO, and Al were taken from the literature [12, 24, 25]. In Fig. 1(a), the lowest unoccupied molecular orbital (LUMO) level of the TFB is sufficiently high to block electrons injected from the cathode through the QDs. Therefore, HODs can be used to characterize the hole carrier transport through the device. Likewise, the valence-band maximum level of ZnO is low enough to block holes injected from the anode, as shown in Fig. 1(b). Through the HODs and the EODs, we were able to compare the hole current and the electron current in V_2O_5/TFB and ZnO, respectively. Figure 1(c) shows the J-V characteristics of HODs based on different TFB concentrations for a fixed concentration of V_2O_5 (1.0 wt.%). The J-V characteristics of EODs (Fig. 1(b))

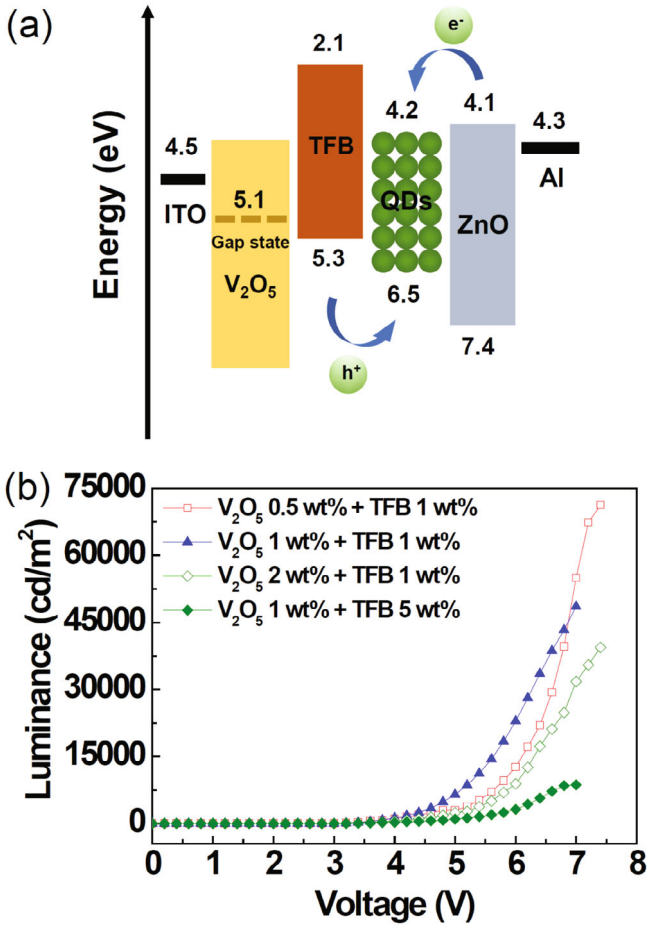

Fig. 2. (Color online) (a) Energy level diagram for the various layers of the QLED. (b) Luminance-voltage (L-V) curves of the QLED devices for four specific cases.

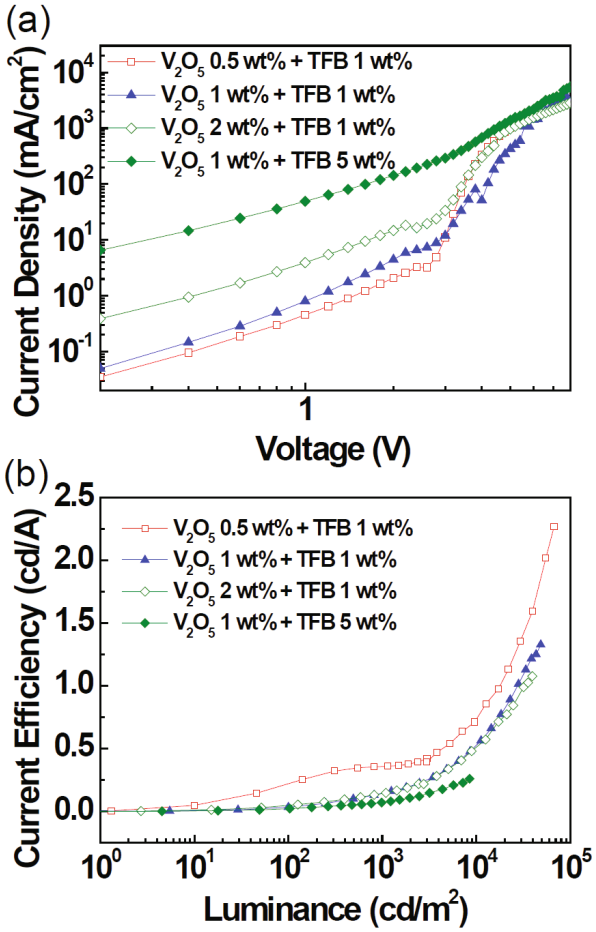

Fig. 3. (Color online) (a) J-V characteristics and (b) current efficiency-luminance characteristics of the QLED devices for four specific cases.

are shown in Fig. 1(c). The current density of the ZnO EOD is more than two orders of magnitude higher than that of the TFB-controlled HOD, which can be explained by considering that the electron mobility of ZnO is higher than that of TFB and that the barrier height between the Al cathode, ZnO, and the QDs is small [26]. As shown in Fig. 1(c), the current density increased as the concentration of TFB decreased, and 1.0 wt.% of TFB showed the highest current density when compared with the other HOD conditions. However, for the HOD with 0.5 wt.% of TFB, the current density was decreased due to the reduced thickness of the TFB layer. Figure 1(d) shows the J-V characteristics of the HODs based on different concentrations of V_2O_5 for a fixed TFB concentration of 1.0wt.%. The HOD with 0.5 wt.% of V_2O_5 exhibited the highest value among the four conditions. Therefore, the most efficient hole injection and transport occurred when 0.5 wt.% of V_2O_5 was used as the HIL and 1.0 wt.% of TFB was used as the HTL.

We fabricated QLED devices with various TFB and V_2O_5 concentrations to confirm the effects of the concentrations of the TFB and the V_2O_5 solutions. The electronic structure of the prepared QLEDs is shown in Fig. 2(a). Gap states are present between the highest occupied molecular orbital (HOMO) and the LUMO of V_2O_5, which originate from oxygen vacancies [27]. The dependence of the luminance on the applied voltage is presented in Fig. 2(b) for various TFB and V_2O_5 concentrations. QLEDs with 0.5 wt.% of V_2O_5 and 1.0 wt.% of TFB showed the highest luminance value of 71,260 cd·m^{-2}, as expected based on the HOD and the EOD study (Fig. 1). Devices with V_2O_5 1.0 wt.% - TFB 1.0 wt.%, V_2O_5 2.0 wt.% - TFB 1.0 wt.%, and V_2O_5 1.0 wt.% - TFB 5.0 wt.% showed 48,570; 39,400; and 8,680 cd·m^{-2}, respectively.

The concentrations of the V_2O_5 and the TFB solution corresponding to the best device performance based on the J-V characteristics of the prepared QLEDs were different from those based on the HOD characterization. The QLED fabricated with 0.5 wt.% of V_2O_5 and 1.0 wt.% of TFB showed the lowest current density, as shown in Fig. 3(a). However, the current density of HODs with 0.5 wt.% of V_2O_5 and 1.0 wt.% of TFB exhibited the highest value as compared with the other HODs made

Table 1. Summary of the electrical characteristics of the QLED devices fabricated by using different concentrations of TFB and V_2O_5.

V_2O_5 concentration	TFB concentration	$V_{turn-on}$ [V]	L_{max} [cd·m^{-2}]	CE [cd·A^{-1}]
1.0 wt%	0.5 wt%	2.2	43,020	1.34
1.0 wt%	1.0 wt%	2.4	48,570	1.52
1.0 wt%	3.0 wt%	2.4	15,330	0.55
1.0 wt%	5.0 wt%	2.6	8,680	0.26
0.5 wt%	1.0 wt%	2.2	71,260	2.27
1.0 wt%	1.0 wt%	2.4	43,350	1.53
1.5 wt%	1.0 wt%	2.4	40,290	1.17
2.0 wt%	1.0 wt%	2.4	39,400	1.08

with different concentrations of V_2O_5 and TFB. This result implies that when the concentration is moderately low, the thickness of the layer is reduced, meaning that the hole injection increases and balances the electron injection from the opposite side. Under this condition, the recombination rate increases, therefore, the current density is reduced in the QLEDs. Due to the increase in the recombination rate, a maximum luminance was observed in QLEDs with 0.5 wt.% of V_2O_5 and 1.0 wt.% of TFB, as shown in Fig. 2(b). Moreover, the highest current efficiency was observed in the same QLEDs due to the reduced current density and increased luminance, as shown in Fig. 3(b). The highest current efficiency was 2.27 cd·A^{-1}. For comparison, the turn-on voltage, maximum luminance, and maximum current efficiency of the QLEDs made under various conditions are summarized in Table 1. The maximum luminance and current efficiency of the QLEDs with 1.0 wt.% of V_2O_5 and 5.0 wt.% of TFB were only 8,680 cd·m^{-2} and 0.26 cd·A^{-1}, respectively. Therefore, the luminance and the current efficiency of the QLEDs were improved when using appropriate concentrations of V_2O_5 and TFB solutions.

The EL spectra of the QLEDs made under different conditions are shown in Fig. 4(a). The working voltage was fixed to 7.2 V. The inset shows the QLED with 0.5 wt.% of V_2O_5 and 1.0 wt.% of TFB in the turn-on state. The EL spectra were consistent with the behaviors presented in Figs. 2 and 3. The peak of the EL spectrum from the QLED made with 0.5 wt.% of V_2O_5 and 1.0 wt.% of TFB was measured to be nine times larger than that of the QLED made with 1.0 wt.% of V_2O_5 and 5.0 wt.% of TFB. The QLED with 0.5 wt.% of V_2O_5 and 1.0 wt.% of TFB featured an emission peak at 525 nm, and the full width at half maximum was 36 nm at 7.2 V. To characterize the green-light emitted from the QLEDs, we plotted the location of each QLED emission on a Commission Internationale de l'Éclairage (CIE) 1931 color space chromaticity diagram, as shown in Fig. 4(b). The CIE coordinate of the QLEDs is (0.17, 0.73), which resides outside the sRGB color gamut. This value has a high color reproducibility for green when compared with

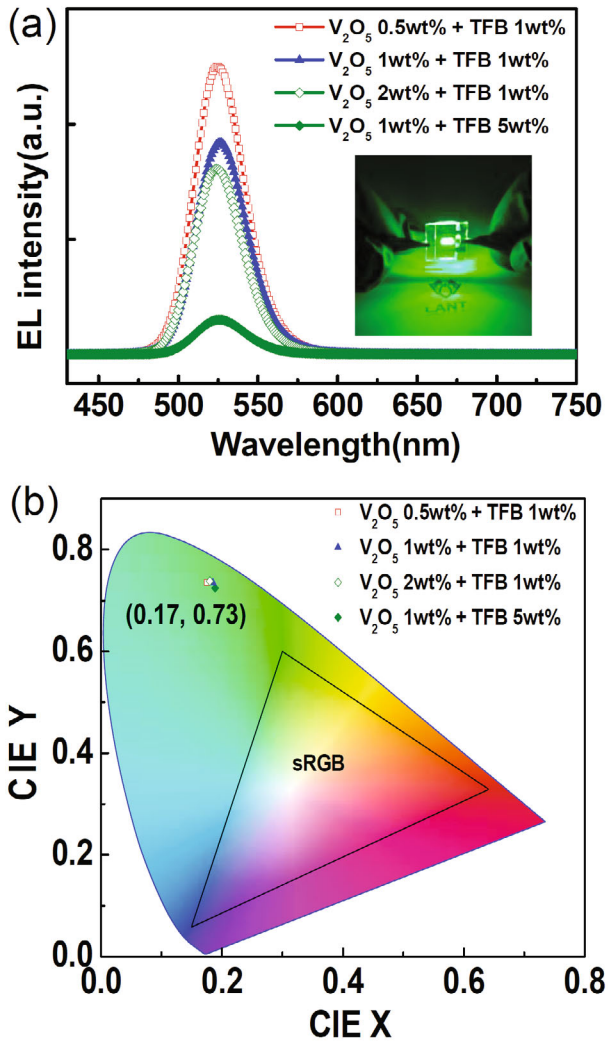

Fig. 4. (Color online) (a) EL spectra of the devices at a driving voltage of 7.2 V. The inset shows the luminance photo of the QLED device (0.5 wt.% V_2O_5 and 1.0 wt.% TFB). (b) The CIE 1931 coordinate corresponding to the EL spectra of the QLED devices in (a).

that of sRGB [28]. The color coordinates of QLEDs made under other conditions were insignificantly different, indicating that the color coordinates barely changed for different concentrations of the V_2O_5 and the TFB solutions.

IV. CONCLUSION

The purpose of this study was to find the optimized concentrations of V_2O_5 for the HIL and TFB for the HTL solutions to increase the hole injection and the luminance of QLEDs. The QLED prepared with 0.5 wt.% of V_2O_5 and 0.1 wt.% of TFB as the HIL and the HTL, respectively, exhibited a maximum current den-

sity of 2.27 cd·A^{-1} and a maximum luminance of 71,260 cd·m^{-2}. At specific concentrations 0.5 wt.% of V_2O_5 and 0.1 wt.% of TFB solutions, the charge balance was improved. Therefore, the hole injection was increased as the recombination of holes and electrons increased. These results should provide useful information for fabricating high-performance QLEDs.

ACKNOWLEDGMENTS

This work was supported by a research project grant from the National Research Foundation of Korea (NRF-2016R1D1A1B03932144).

REFERENCES

[1] H. Shen *et al.*, Nat. Photonics **13**, 192 (2019).
[2] Y. Wei *et al.*, Adv. Funct. Mater. **28**, 1706690 (2018).
[3] Z. Pan *et al.*, Chem. Soc. Rev. **47**, 7659 (2018).
[4] H. Schlicke *et al.*, in *2018 IEEE 13th Nanotechnology Materials and Devices Conference* (Oregon, USA, October 14–17, 2018), p. 1.
[5] S. A. Empedocles and M. G. Bawendi, Science **278**, 2114 (1997).
[6] F. Yuan *et al.*, Nat. Commun. **9**, 2249 (2018).
[7] Y. Zou *et al.*, Adv. Funct. Mater. **27**, 1603325 (2017).
[8] M. K. Choi, J. Yang, T. Hyeon and D. H. Kim, NPJ Flexible Electron. **2**, 10 (2018).
[9] K. H. Lee *et al.*, Nanoscale **10**, 6300 (2018).
[10] Y. Zhang *et al.*, Org. Electron. **44**, 189 (2017).
[11] H. Zhang, S. Wang, X. Sun and S. Chen, J. Mater. Chem. C **5**, 817 (2017).
[12] S. B. Heo, M. J. Kim, J. H. Yu and S. J. Kang, Curr. Appl. Phys. **19**, 657 (2019).
[13] Z. Li, Microelectron. Int. **35**, 215 (2018).
[14] J. A. R. Dimmock, E. A. Boardman and T. M. Smeeton, Dig. Tech. Pap. **50**, 648 (2019).
[15] G. Sarasqueta, K. R. Choudhury, J. Subbiah and F. So, Adv. Funct. Mater. **21**, 167 (2011).
[16] X. Dai *et al.*, Nature **515**, 96 (2014).
[17] F. Wang *et al.*, J. Phys. Chem. Lett. **10**, 960 (2019).
[18] B. S. Mashford *et al.*, Nat. Photon. **7**, 407 (2013).
[19] D. Bozyigit, O. Yarema and V. Wood, Adv. Funct. Mater. **23**, 3024 (2013).
[20] J. Pan *et al.*, RSC Adv. **7**, 43366 (2017).
[21] F. Cao *et al.*, Adv. Funct. Mater. **27**, 1704278 (2017).
[22] Z. Li, Vacuum **137**, 38 (2017).
[23] D. H. Song *et al.*, RSC Adv. **7**, 43396 (2017).
[24] S. A. Choulis *et al.*, Adv. Funct. Mater. **16**, 1075 (2006).
[25] M. Uda, A. Nakamura, T. Yamamoto and Y. Fujimoto, J. Electron. Spectros. Relat. Phenomena **88**, 643 (1998).
[26] J. Yang *et al.*, Diam. Relat. Mater. **73**, 154 (2017).
[27] S. M. Lee *et al.*, Curr. Appl. Phys. **17**, 442 (2017).
[28] E. Jang *et al.*, Adv. Mater. **22**, 3076 (2010).